

第八讲：粘性流动数值解

Chapter 20 Navier-Stokes Solutions: Some Examples

Lecturer: Ao Xu (徐翱)

Email: axu@nwpu.edu.cn

Office: 航空楼A501

School of Aeronautics

A numerical simulation of the flow over an airfoil using the Reynolds averaged Navier-Stokes equations can be conducted on today's supercomputers in less than a half hour for less than \$1000 cost in computer time. If just one such simulation had been attempted 20 years ago on computers of that time (e.g., the IBM 704 class) and with algorithms then known, the cost in computer time would have amounted to roughly \$10 million, and the results for that single flow would not be available until 10 years from now, since the computation would have taken about 30 years to complete.

Dean R. Chapman, NASA, 1977

利用雷诺平均navier-stokes方程对翼型上的流动进行数值模拟，可以在今天的超级计算机上以不到1000美元的计算机时间在不到半小时内进行。如果20年前在当时的计算机（如IBM 704类）上仅尝试过一次这样的模拟，并且使用当时已知的算法，计算机时间成本将达到大约1000万美元，并且直到10年后才能获得单一流程的结果，因为计算大约需要30年时间。

第一节：引言

19.1 INTRODUCTION

粘性流动求解的一种方法：

Navier-Stokes equations 的数值计算

The solution of viscous flows

We have the following options:

1. Exact solution
2. Approximate solution
3. Direct numerical simulation

- Its purpose is to discuss the third option for the solution of viscous flows, the exact numerical solution of the complete Navier-Stokes equations.
- This option is the purview of modern computational fluid dynamics—it is a state-of-the-art research activity which is currently in a rapid state of development.
- This subject now occupies volumes of modern literature.

大规模并行计算

国家超级计算无锡中心，拥有世界上首台峰值运算性能超过每秒十亿亿次浮点运算能力的超级计算机——“神威·太湖之光”。该系统是我国“十二五”期间“863计划”的重大科研成果，由国家并行计算机工程技术研究中心研制，运算系统全面采用了由国家高性能集成电路设计中心通过自主核心技术研制的国产“**申威26010**”众核处理器。



Summit (Top 1, Nov. 2019)

Oak Ridge National Laboratory, USA

第二节：数值方法

20.2 THE APPROACH

微分形式的粘性流动控制方程 (Navier-Stokes equations)

连续方程:

$$\frac{\partial \rho}{\partial t} = - \left[\frac{\partial(\rho u)}{\partial x} + \frac{\partial(\rho v)}{\partial y} + \frac{\partial(\rho w)}{\partial z} \right]$$

动量方程:

$$\frac{\partial u}{\partial t} = -u \frac{\partial u}{\partial x} - v \frac{\partial u}{\partial y} - w \frac{\partial u}{\partial z} + \frac{1}{\rho} \left[-\frac{\partial p}{\partial x} + \frac{\partial \tau_{xx}}{\partial x} + \frac{\partial \tau_{yx}}{\partial y} + \frac{\partial \tau_{zx}}{\partial z} \right]$$

$$\frac{\partial v}{\partial t} = -u \frac{\partial v}{\partial x} - v \frac{\partial v}{\partial y} - w \frac{\partial v}{\partial z} + \frac{1}{\rho} \left[-\frac{\partial p}{\partial y} + \frac{\partial \tau_{xy}}{\partial x} + \frac{\partial \tau_{yy}}{\partial y} + \frac{\partial \tau_{zy}}{\partial z} \right]$$

$$\frac{\partial w}{\partial t} = -u \frac{\partial w}{\partial x} - v \frac{\partial w}{\partial y} - w \frac{\partial w}{\partial z} + \frac{1}{\rho} \left[-\frac{\partial p}{\partial z} + \frac{\partial \tau_{xz}}{\partial x} + \frac{\partial \tau_{yz}}{\partial y} + \frac{\partial \tau_{zz}}{\partial z} \right]$$

能量方程:

$$\begin{aligned} \frac{\partial(e + V^2/2)}{\partial t} = & -u \frac{\partial(e + V^2/2)}{\partial x} - v \frac{\partial(e + V^2/2)}{\partial y} - w \frac{\partial(e + V^2/2)}{\partial z} + \dot{q} \\ & + \frac{1}{\rho} \left[\frac{\partial}{\partial x} \left(k \frac{\partial T}{\partial x} \right) + \frac{\partial}{\partial y} \left(k \frac{\partial T}{\partial y} \right) + \frac{\partial}{\partial z} \left(k \frac{\partial T}{\partial z} \right) \right. \\ & - \frac{\partial(pu)}{\partial x} - \frac{\partial(pv)}{\partial y} - \frac{\partial(pw)}{\partial z} + \frac{\partial(u\tau_{xx})}{\partial x} \\ & + \frac{\partial(u\tau_{yx})}{\partial y} + \frac{\partial(u\tau_{zx})}{\partial z} + \frac{\partial(v\tau_{xy})}{\partial x} + \frac{\partial(v\tau_{yy})}{\partial y} + \frac{\partial(v\tau_{zy})}{\partial z} \\ & \left. + \frac{\partial(w\tau_{xz})}{\partial x} + \frac{\partial(w\tau_{yz})}{\partial y} + \frac{\partial(w\tau_{zz})}{\partial z} \right] \end{aligned}$$

低速非定常粘性流动方程的特性：

- These equations have been written with the time derivatives on the left-hand side and all spatial derivatives on the right-hand side.
- This is the form suitable to a time-dependent solution of the equations.
- Indeed, Equations are partial differential equations that have a mathematically “elliptic” behavior; that is, on a physical basis they treat flow field information and flow disturbances that can travel throughout the flow field, in both the upstream and downstream directions.
- The time-dependent technique is particularly suited to such a problem.

流场数值计算方法：

➤ 网格生成：

将连续的几何空间求解区域划分为离散的网格节点。

➤ 空间差分：

采用适当的差分格式代替微分方程中的空间偏导数，将微分方程离散成差分方程。

$$\left(\frac{\partial u}{\partial x}\right)_{i,j} = \frac{u_{i+1,j} - u_{i,j}}{\Delta x}$$

➤ 湍流模型：

根据湍流的特性和数值模拟精度的要求选择不同的湍流模型，并进行相应的离散计算，例如最简单的B-L代数模型。

➤ 时间推进：

采用相应的时间差分格式（隐式或显式），按照时间先后顺序推进求解整个非定常流动过程。

MacCormack 方法（预估—修正方法）

$$\left(\frac{\partial u}{\partial t}\right)_{i,j} = \frac{u_{i,j}^{t+\Delta t} - u_{i,j}^t}{\Delta t}$$

第三节：典型流动の数値解

20.3 EXAMPLES OF SOME SOLUTIONS

数值计算方法

1. They were obtained by means of a time-dependent solution using MacCormack's technique.
2. They utilize the Baldwin-Lomax turbulence model, turbulent flow is modeled in these calculations.
3. They require anywhere from thousands to close to a million grid points for their solution.
4. Therefore, these are problems that must be solved on large-scale digital computers ???

后台阶绕流 Flow over a Rearward-Facing Step

来流条件: $M=2.19$ 、 $Re=70,000$, 速度场分布图

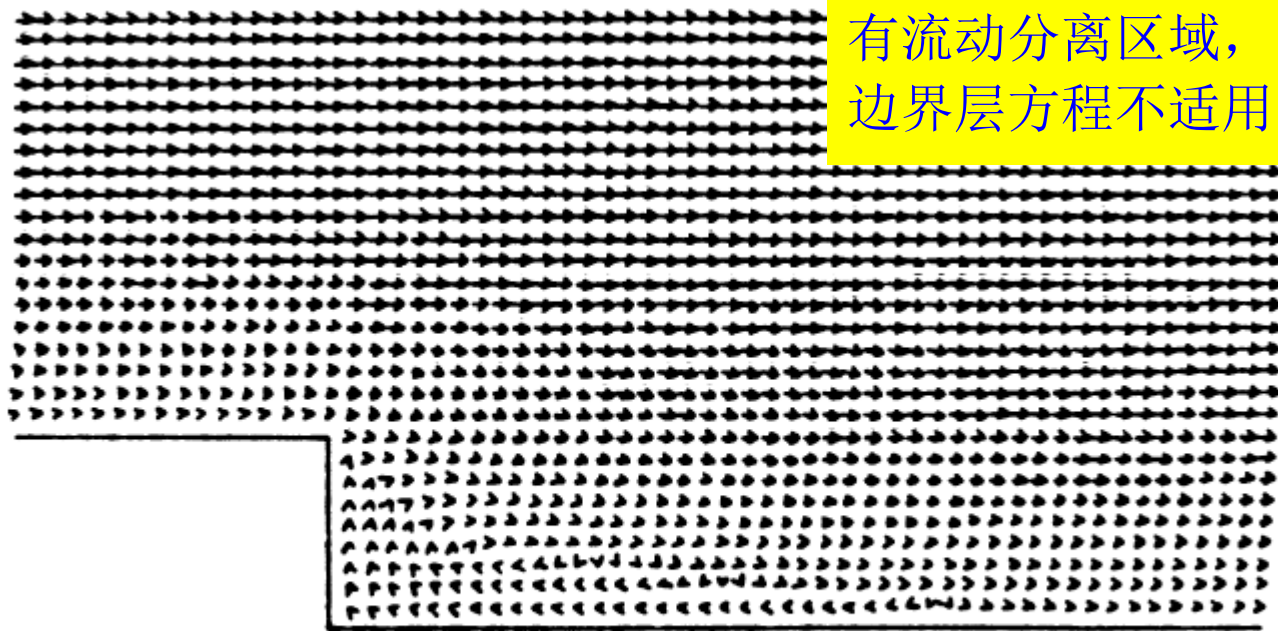


Figure 20.1 Velocity vector diagram for the flow over a rearward-facing step. $M = 2.19$, $T = 1005$ K, $Re = 70,000$ (based on step height) (Reference 46). Note the recirculating flow region downstream of the step.

后台阶绕流 Flow over a Rearward-Facing Step

来流条件: $M=2.19$ 、 $Re=70,000$, 温度场分布图

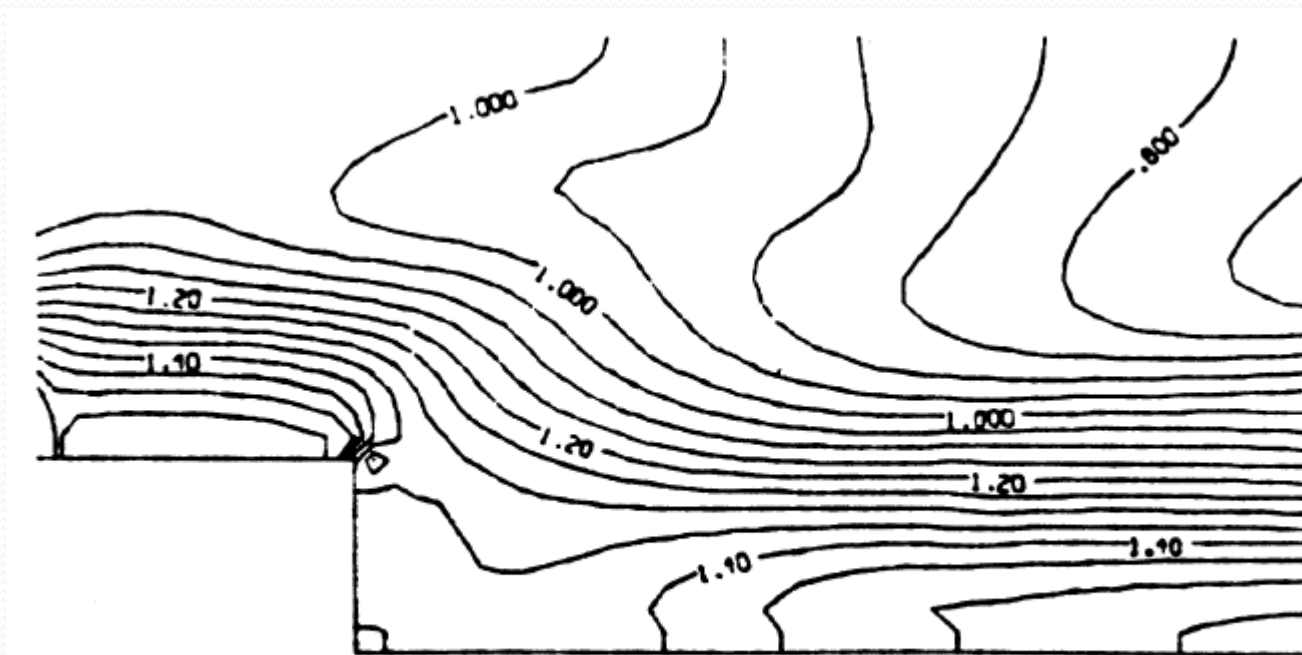
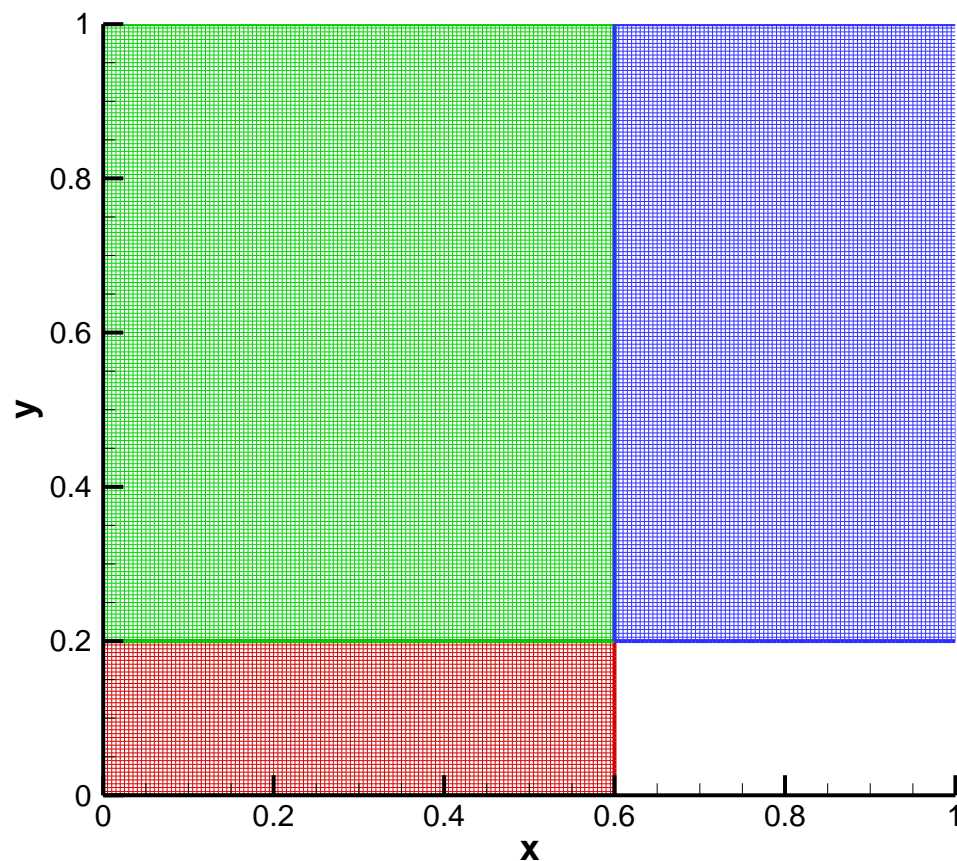


Figure 20.2 Temperature contours for the flow shown in Figure 20.1. The separated region just downstream of the step is a reasonably constant pressure, constant temperature region.

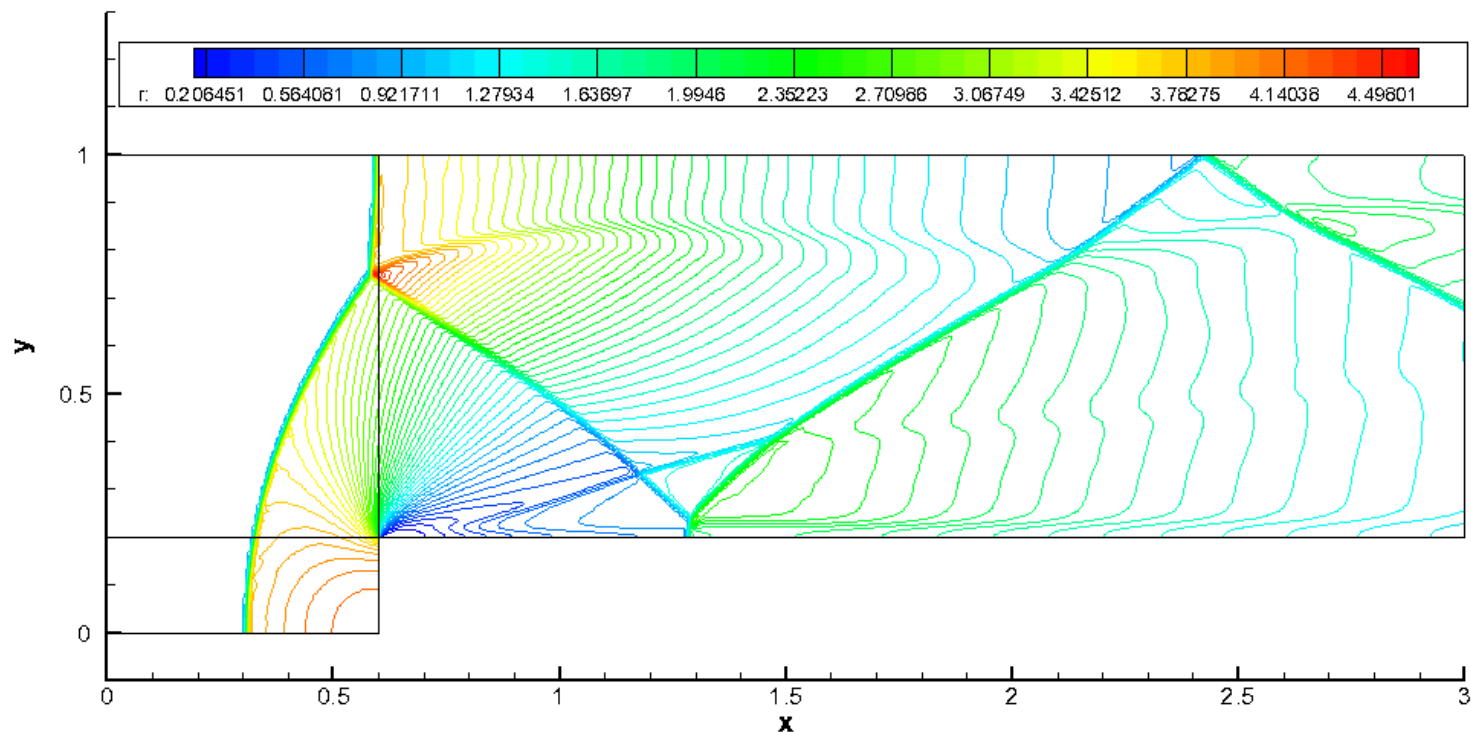
前台阶绕流 Flow over a Forward-Facing Step

来流条件: $M=3.0$, 计算网格分布 $\Delta x = \Delta y = 1/200$



前台阶绕流 Flow over a Forward-Facing Step

来流条件: $M=3.0$, 密度等值线图



翼型绕流 Flow over an Airfoil

来流条件: $M=0.5$, $Re=100,000$, 贴体网格分布

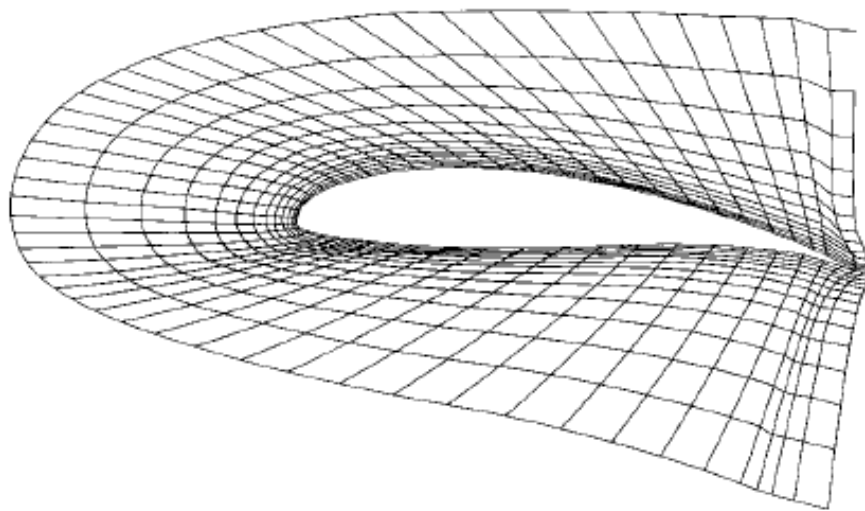


Figure 20.3 Curvilinear, boundary-fitted finite-difference grid for the solution of the flow over an airfoil.
(Data Source: Kothari and Anderson, Reference 56.)

翼型绕流 Flow over an Airfoil

来流条件: $M=0.5$, $Re=100,000$, 流线分布, 层流和湍流

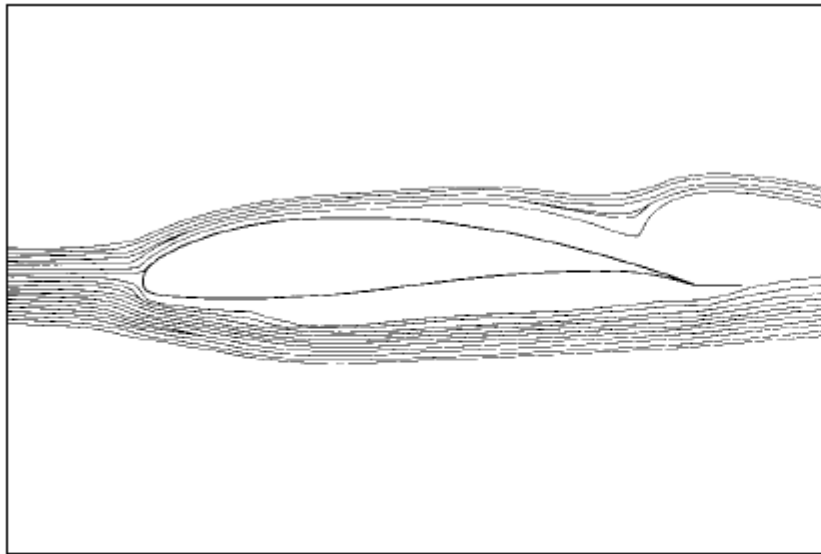
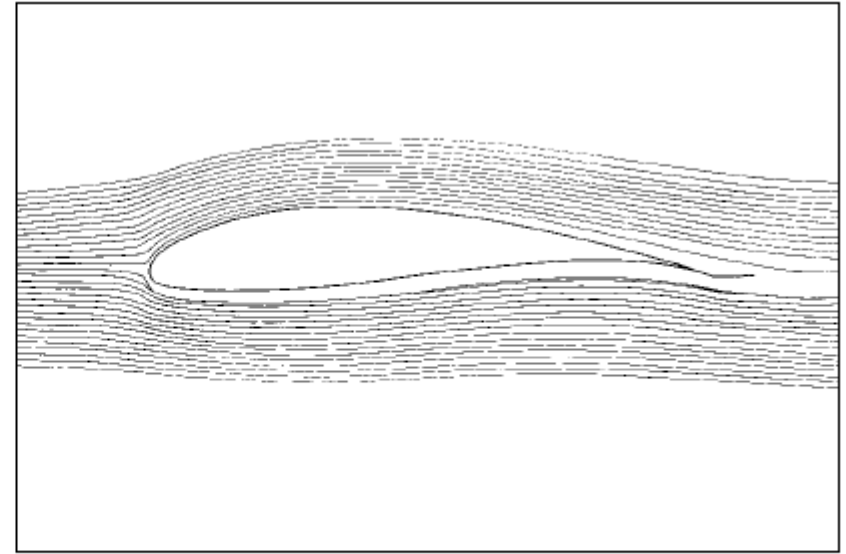


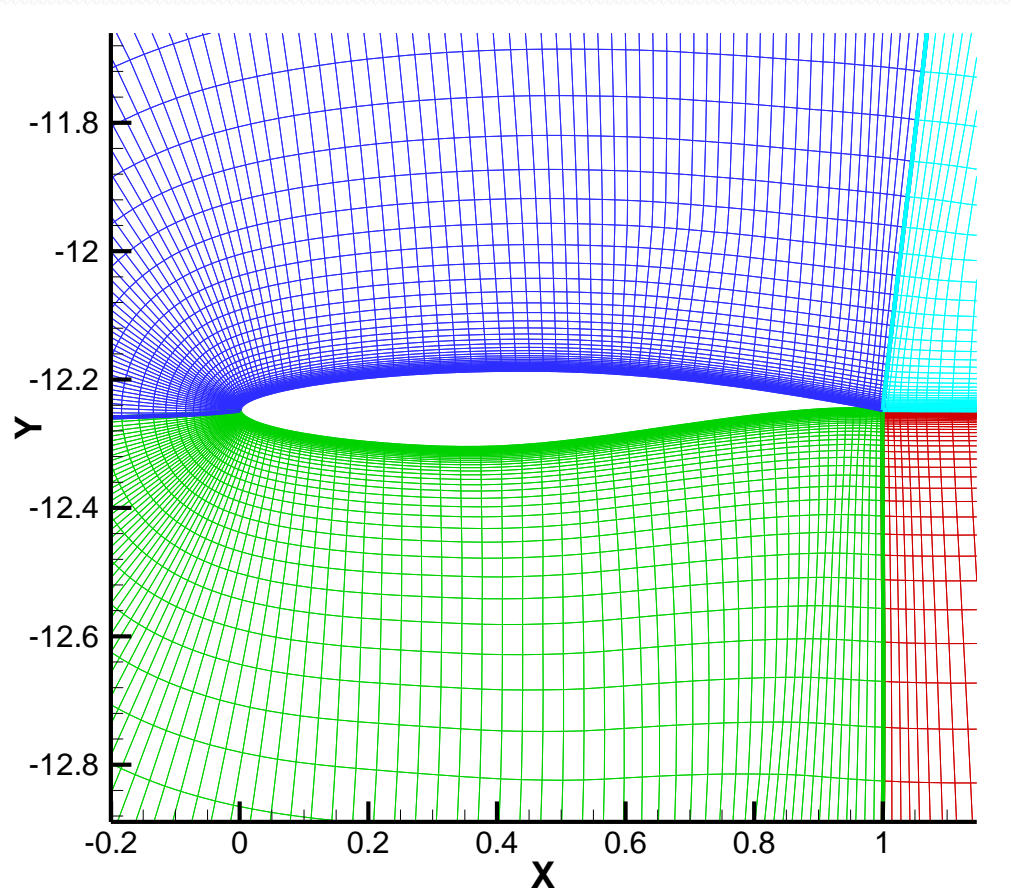
Figure 20.4 Streamlines for the low Reynolds flow over a Wortmann airfoil. $Re = 100,000$. (a) Laminar flow.



(b) Turbulent flow. (Data Source: Kothari and Anderson, Reference 56.)

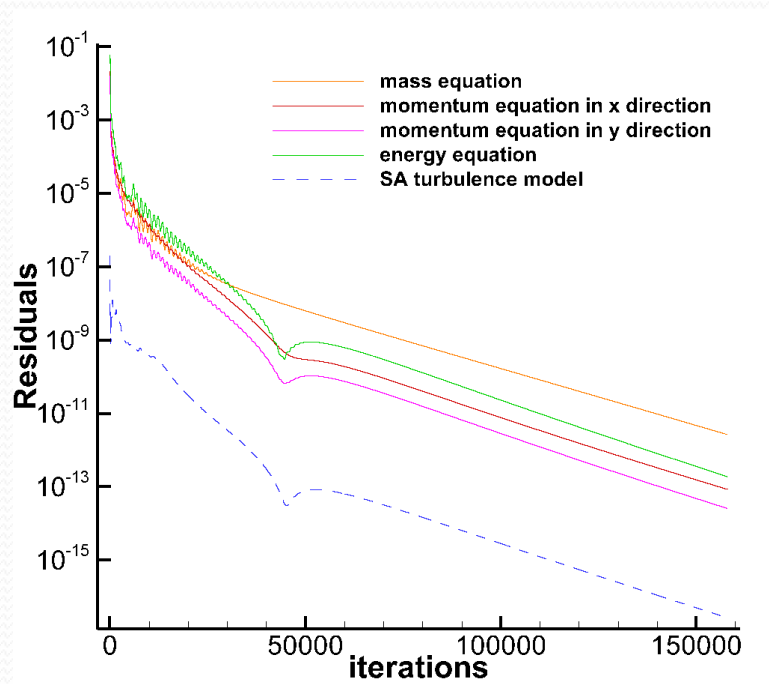
翼型绕流 Flow over an Airfoil RAE2822翼型

来流条件: $M=0.75$, $Re=6200,000$, $\alpha=2.72$, 贴体网格分布: 257×97

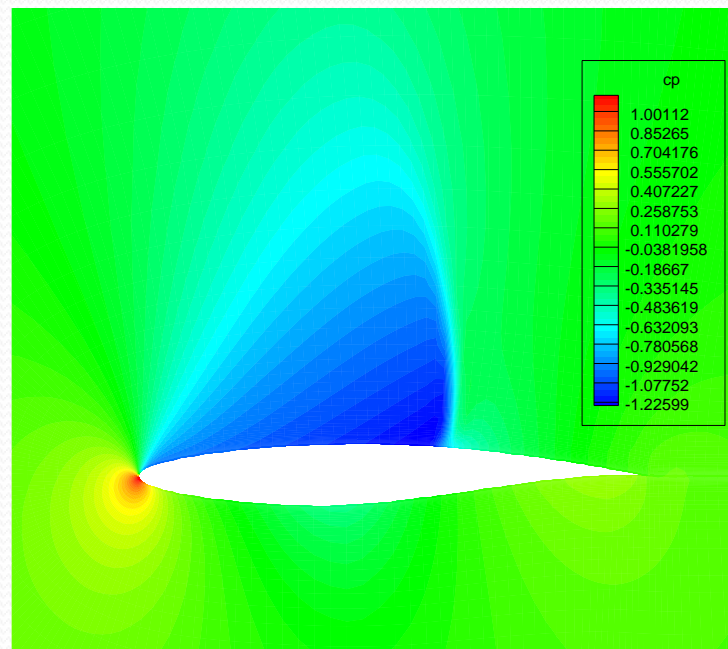


翼型绕流 Flow over an Airfoil RAE2822翼型

来流条件: $M=0.75$, $Re=6200,000$, $\alpha=2.72^\circ$, SA湍流模型



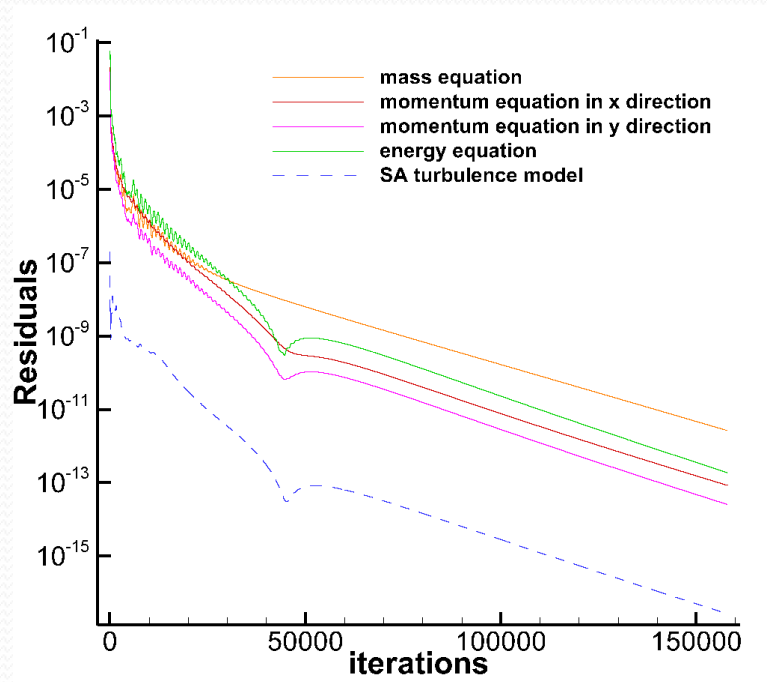
残值收敛曲线



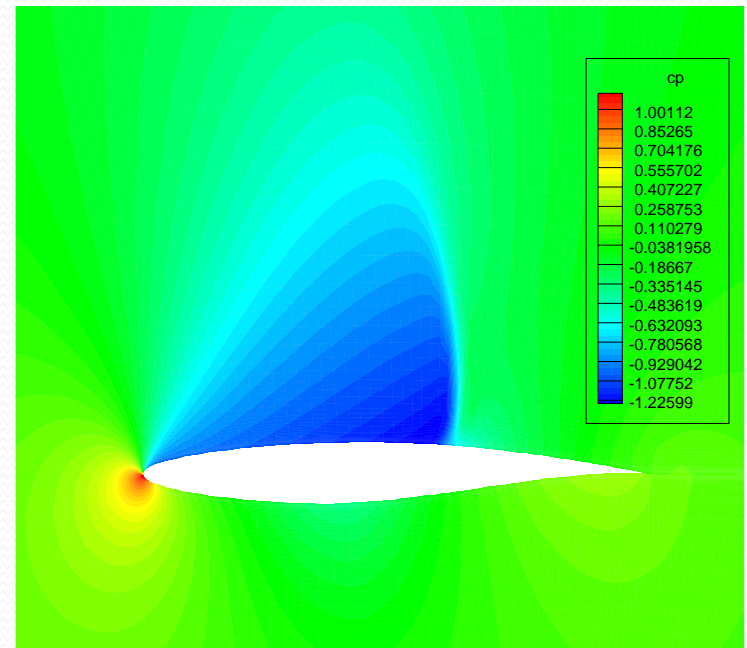
翼型表面压力分布

翼型绕流 Flow over an Airfoil RAE2822翼型

来流条件: $M=0.75$, $Re=6200,000$, $\alpha=2.72$, 贴体网格分布: 257×97



残值收敛曲线



翼型表面压力分布

全机绕流 Flow over a Complete Airplane

We end this section by noting a history-making calculation. To illustrate the results, the surface streamline pattern for X-24C.

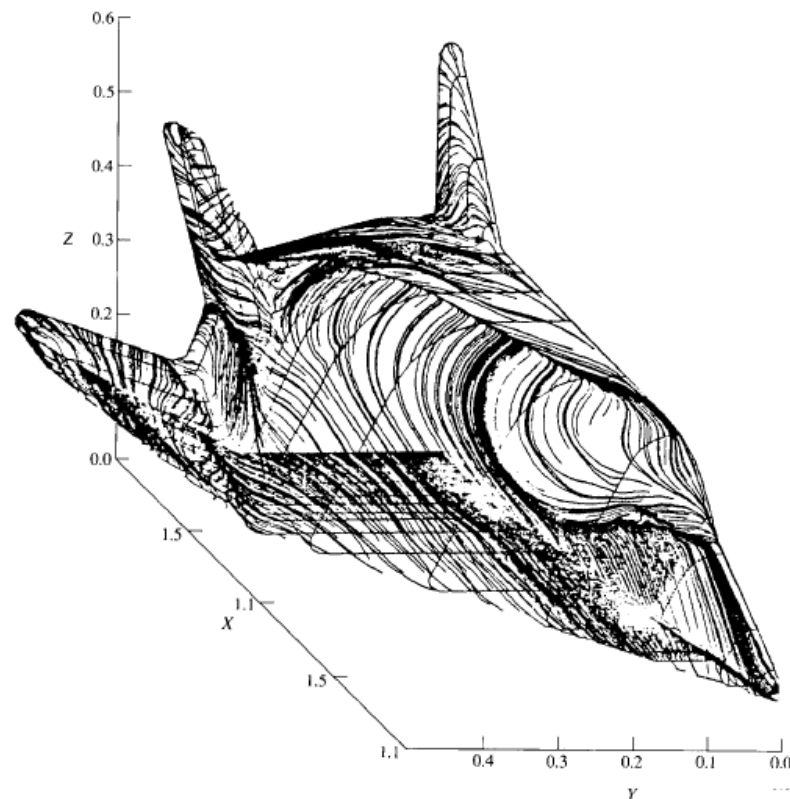
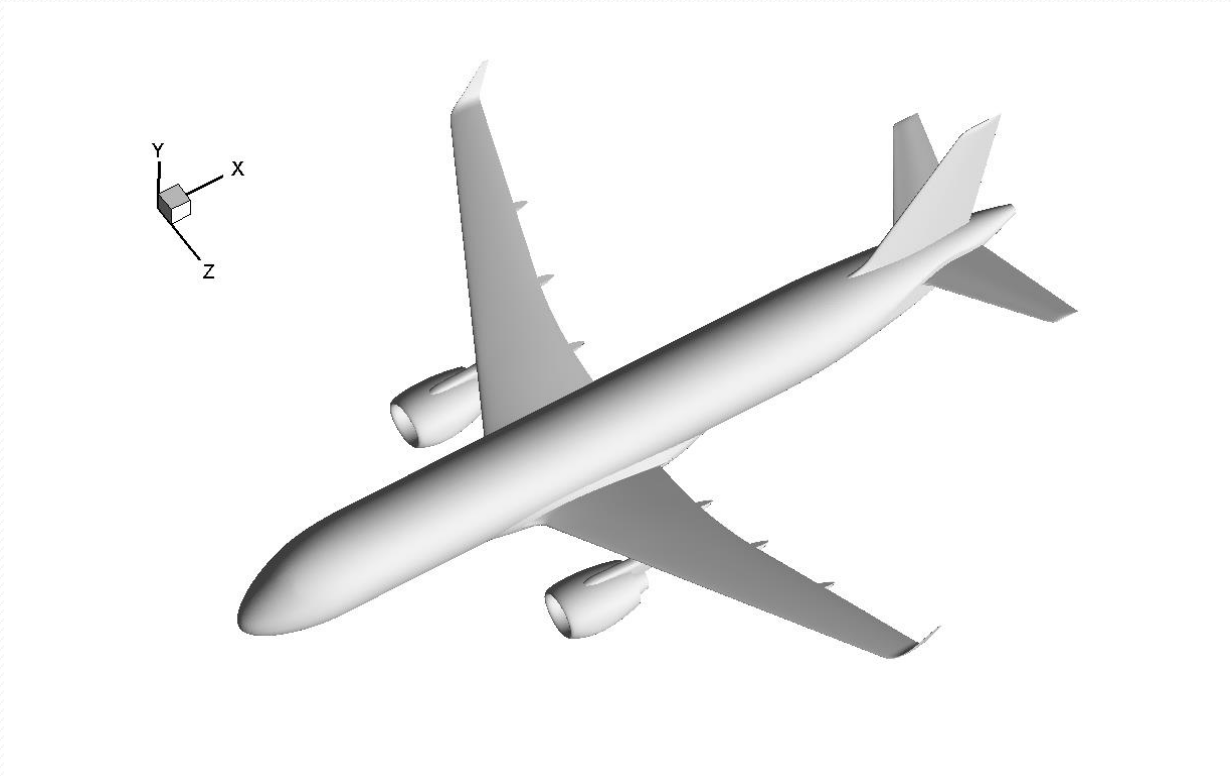


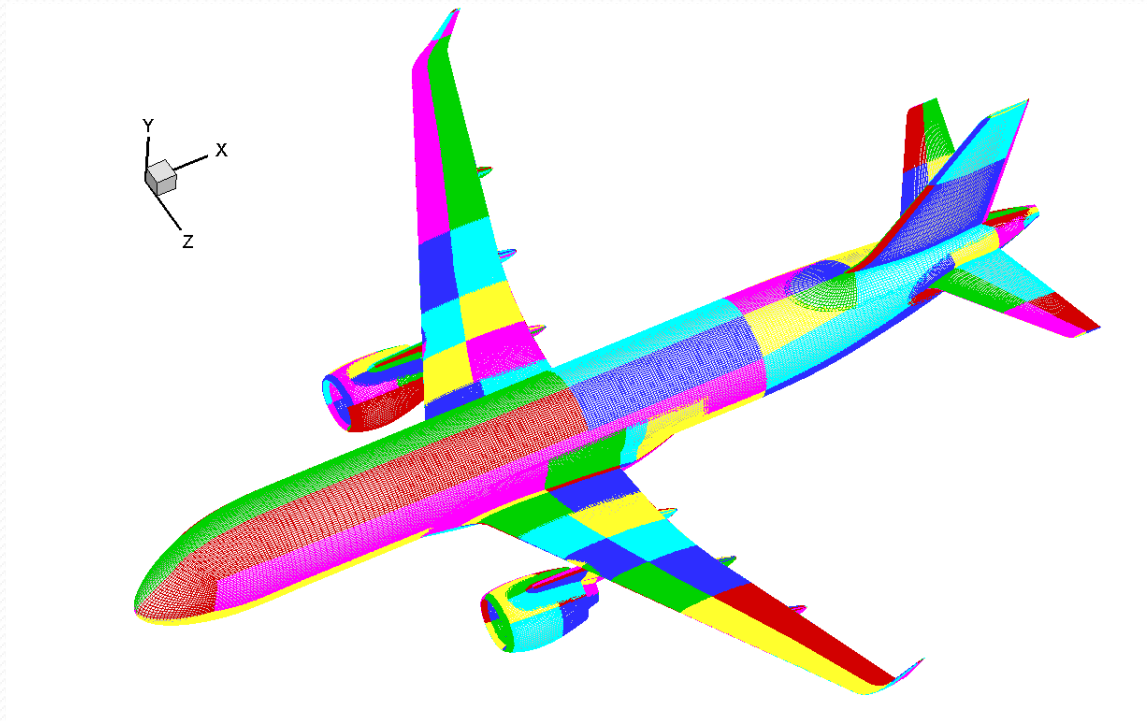
Figure 20.5 Surface shear stress lines on the X-24C. (Data Source: Shang and Scherr, Reference 57.)

全机绕流 Flow over a Complete Airplane



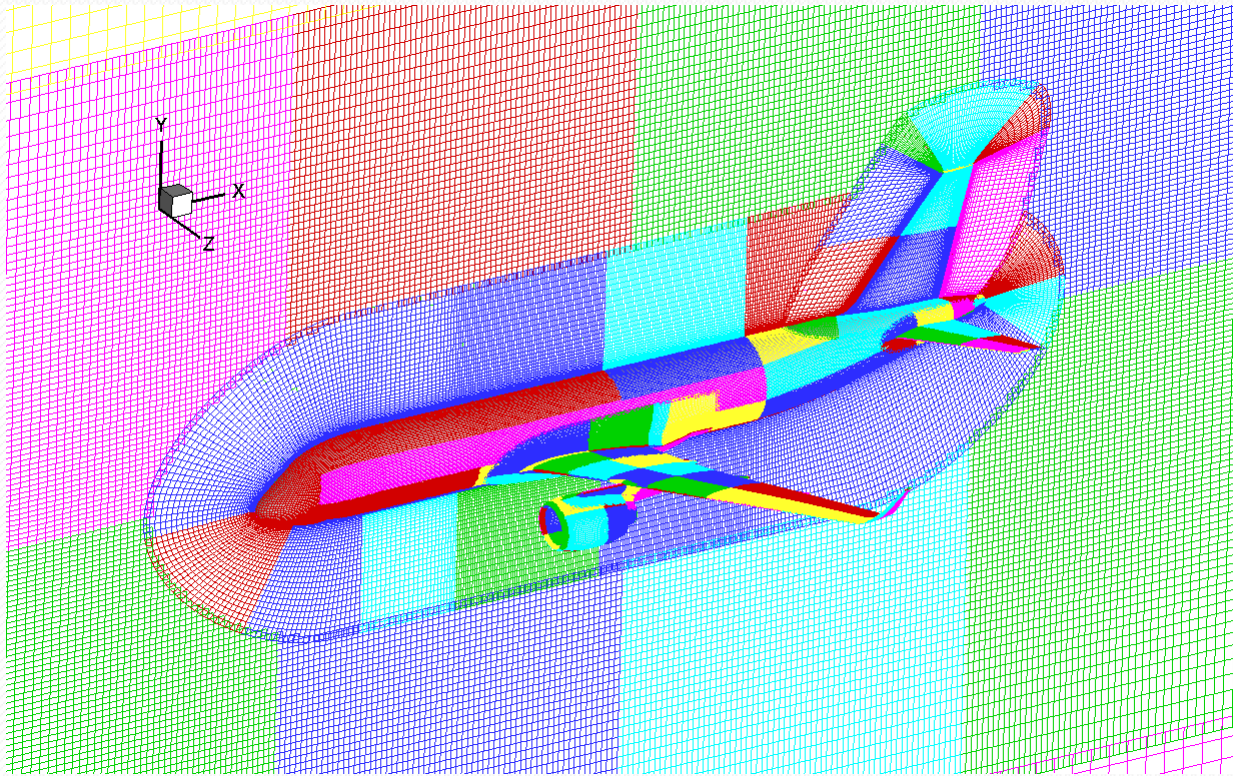
中国商飞COMAC C919全机模型

全机绕流 Flow over a Complete Airplane



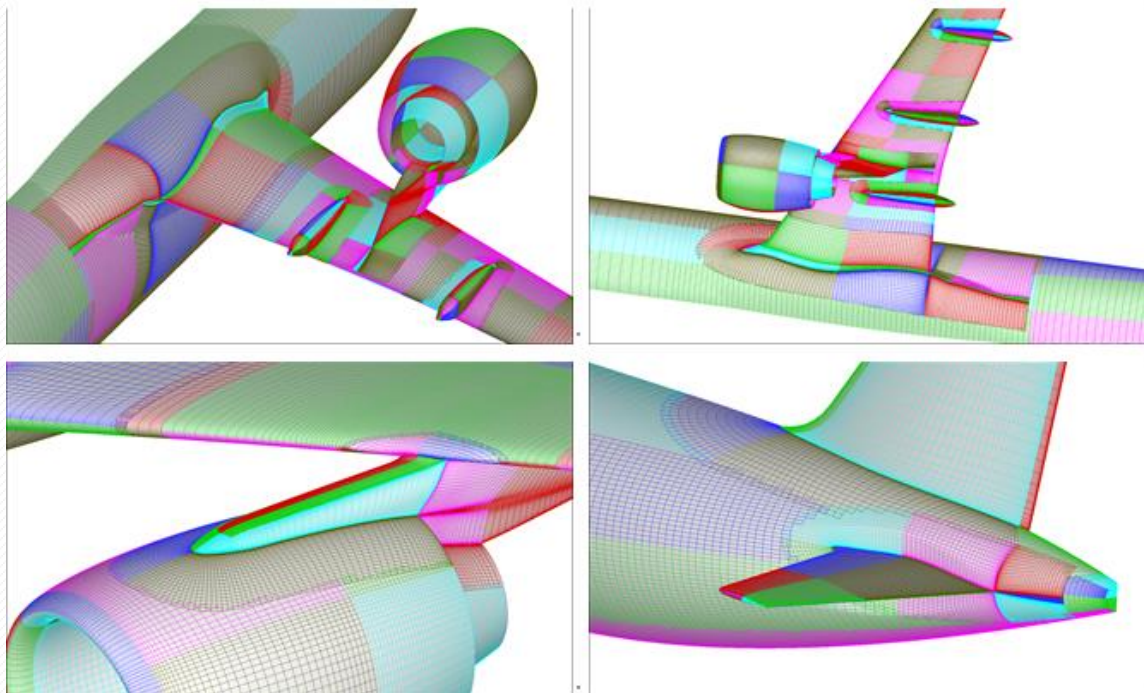
机体表面多层多块隐式嵌套重叠网格，8千万网格单元

全机绕流 Flow over a Complete Airplane



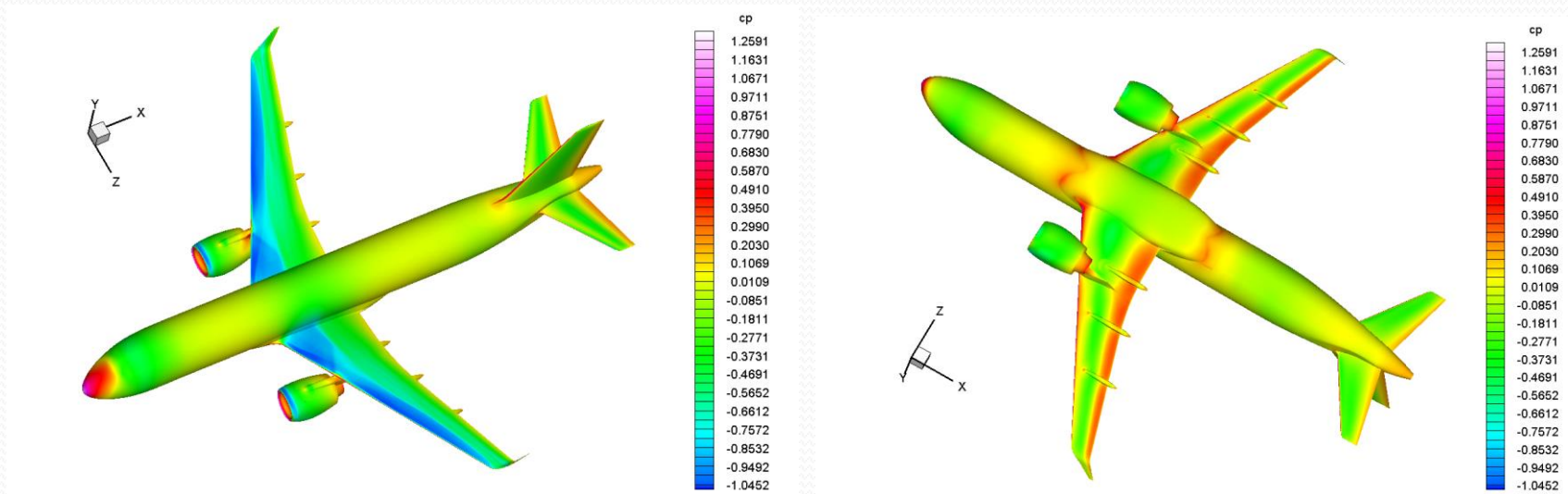
机体表面多层多块隐式嵌套重叠网格

全机绕流 Flow over a Complete Airplane



机体表面多层多块隐式嵌套重叠网格

全机绕流 Flow over a Complete Airplane



C919机体表面压力分布云图，马赫数0.785，迎角2.62度

激波边界层干扰 Shock-Wave/Boundary-Layer Interaction

激波引起边界层分离

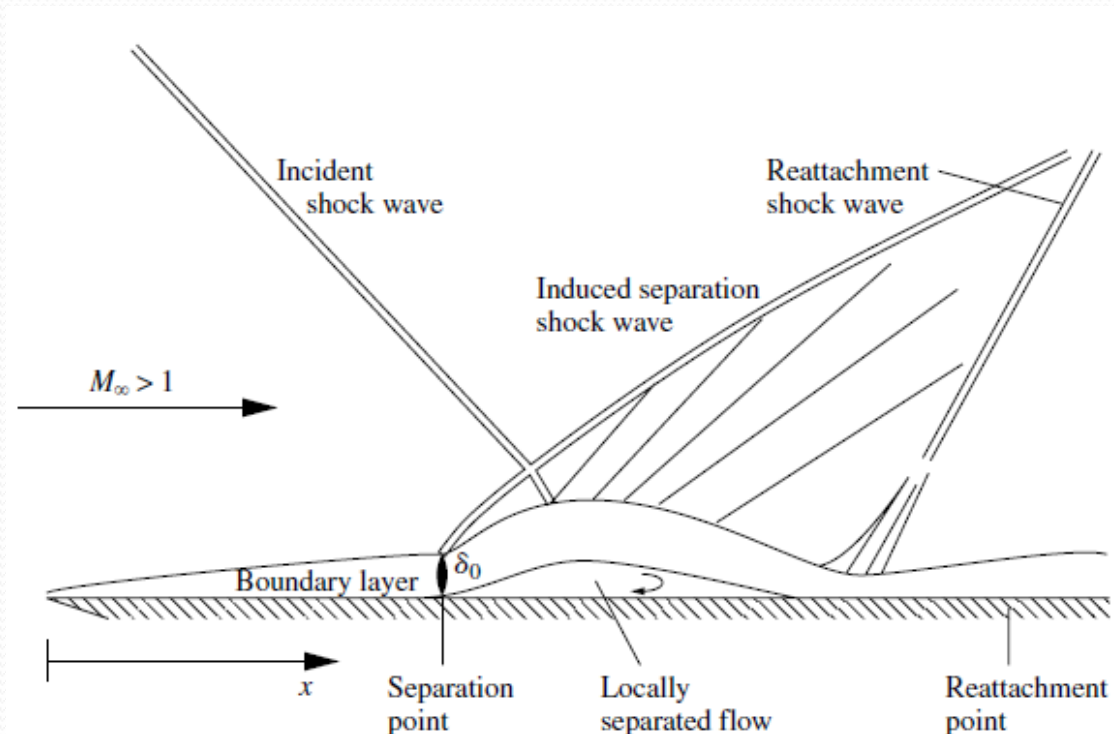


Figure 20.6 Schematic of the shock-wave/boundary-layer interaction.

激波边界层干扰 Shock-Wave/Boundary-Layer Interaction

M=3.0 激波引起边界层分离，壁面压力与摩擦力分布

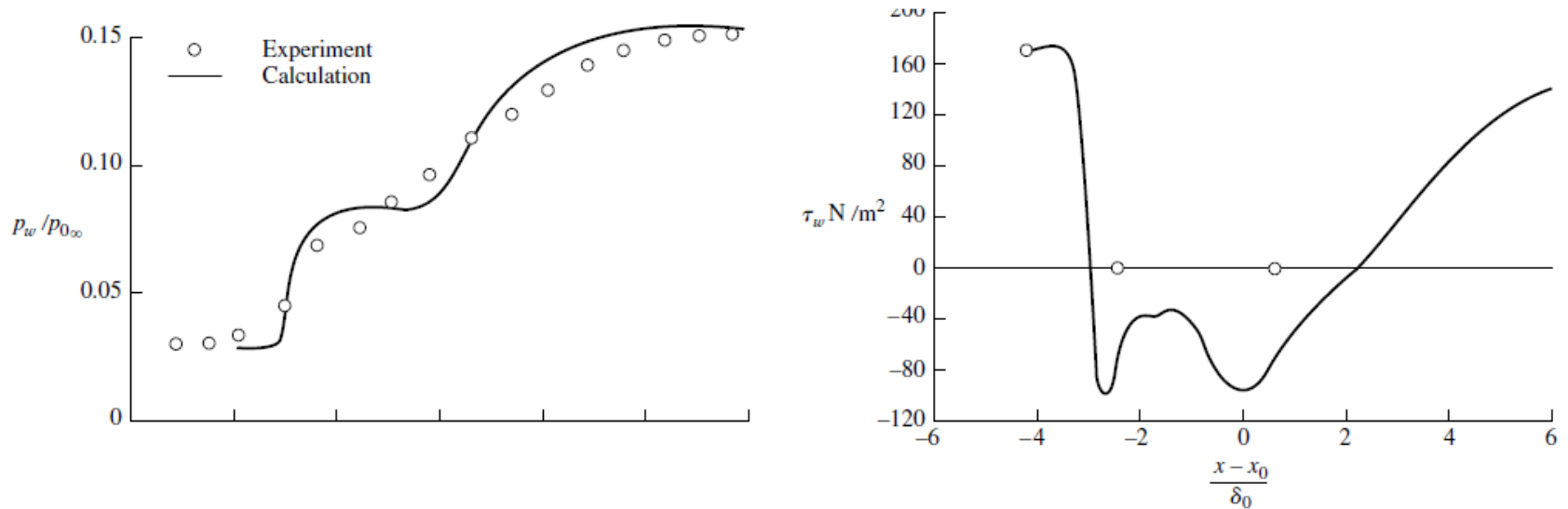


Figure 20.7 Effects of shock-wave/boundary-layer interaction on (a) pressure distribution, and (b) shear stress for Mach 3 turbulent flow over a flat plate.

带凸起的翼型绕流

Flow over an Airfoil with a Protuberance

$M=0.15$, $Re=1500,000$, NACA 0015, OVERFLOW

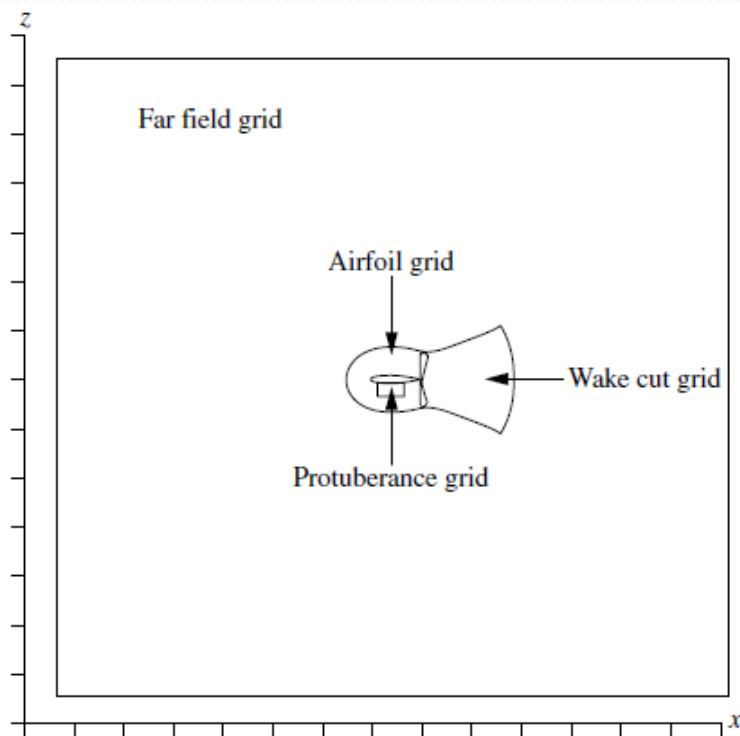


Figure 20.8 Individual grid boundary outlines used in the chimera grid scheme for calculating the flow over an airfoil with a protuberance.

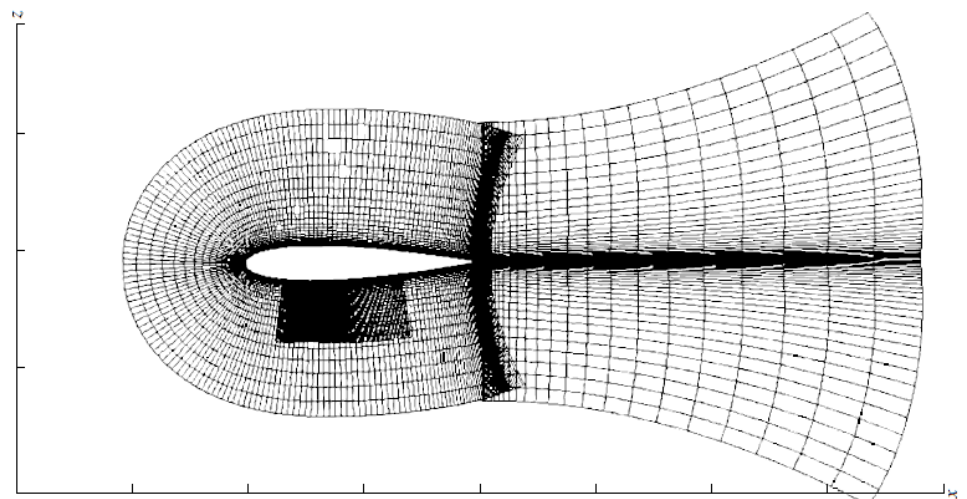


Figure 20.9 Zoom view of the airfoil, wake cut, and protuberance grids.

带凸起的翼型绕流

Flow over an Airfoil with a Protuberance

$M=0.15$, $Re=1500,000$, NACA 0015, OVERFLOW

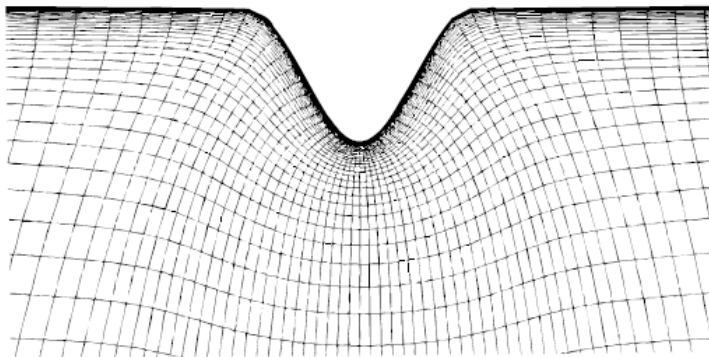


Figure 20.11 A detail of the grid in the vicinity of the protuberance.

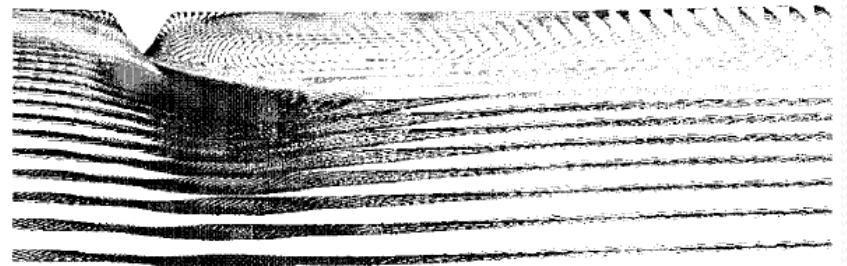


Figure 20.12 Computed velocity vector field around and downstream of the protuberance.

带凸起的翼型绕流

Flow over an Airfoil with a Protuberance

$M=0.15$, $Re=1500,000$, NACA 0015, OVERFLOW

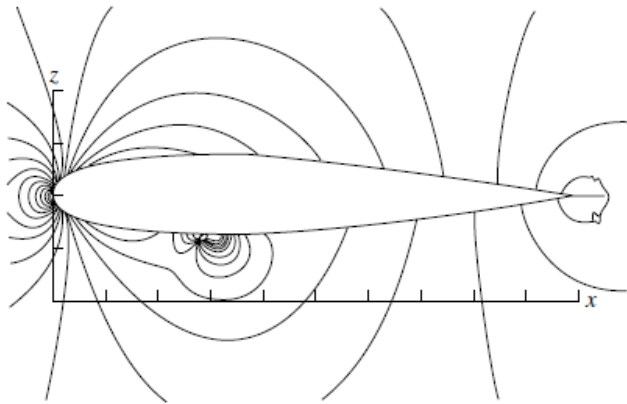


Figure 20.13 Computed pressure contours around the NACA 0012 airfoil with a protuberance.



Figure 20.14 Streamline pattern over the bottom of an NACA 0012 airfoil, over which a series of jets is distributed which are alternatively blowing or sucking mass into or out of the flow, with the overall net mass injected into the flow being zero—a zero-mass jet array. (Data Source: Hassan and JanakiRam, Reference 91.)

第四节：摩擦阻力计算精度问题

20.4 THE ISSUE OF ACCURACY FOR THE PREDICTION OF SKIN FRICTION DRAG

阻力的计算方法

- The aerodynamic drag on a body is the sum of pressure drag and skin friction drag.
- For attached flows, the pressure drag can be obtained from inviscid flow analyses.
- Today the only viable and general method of the analysis of pressure drag for such flows is a complete numerical Navier-Stokes solution.
- The prediction of skin friction on the surface of a body in an attached flow is nicely accomplished by means of a boundary-layer solution coupled with an inviscid flow analysis to define the flow conditions at the edge of the boundary layer.
- However, as mentioned above, if regions of flow separation are present, a full Navier-Stokes solution can be used to obtain local skin friction and heat transfer.

数值方法精度的影响因素

$$\begin{array}{l} \text{速度型} \rightarrow \left(\frac{\partial u}{\partial y}\right)_w \rightarrow \tau_w = \mu \left(\frac{\partial u}{\partial y}\right)_w \longrightarrow c_f = \frac{\tau_w}{\rho_e u_e^2 / 2} \\ \text{温度型} \rightarrow \left(\frac{\partial T}{\partial y}\right)_w \rightarrow \dot{q}_w = -k \left(\frac{\partial T}{\partial y}\right)_w \longrightarrow C_H = \frac{\dot{q}_w}{\rho_e u_e (h_{aw} - h_w)} \end{array}$$

对于复杂流动问题（流动分离）：

- (1) 需要在近物面处布置非常密的网格
- (2) 考虑湍流模型计算精度的影响
- (3) 大多数湍流模型缺乏对转捩的预测能力

湍流模型对计算结果的影响

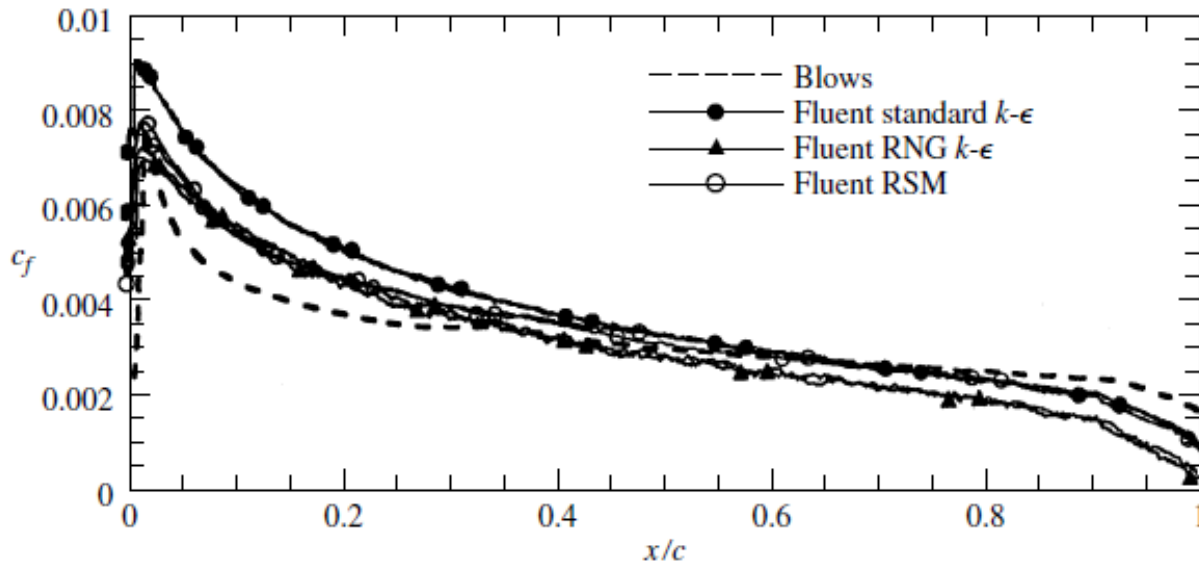


Figure 20.15 Distribution of the skin-friction coefficient over the surface of an NACA 0012 airfoil at zero angle of attack in low-speed flow. Comparison of three Navier-Stokes calculations using different turbulent models, and results obtained from a boundary-layer calculation. The boundary-layer results are given by the dashed curve labeled “Blows.” (Data Source: Lombardi, Salvetti, and Pinelli, Reference 92.)

数值方法对计算结果的影响

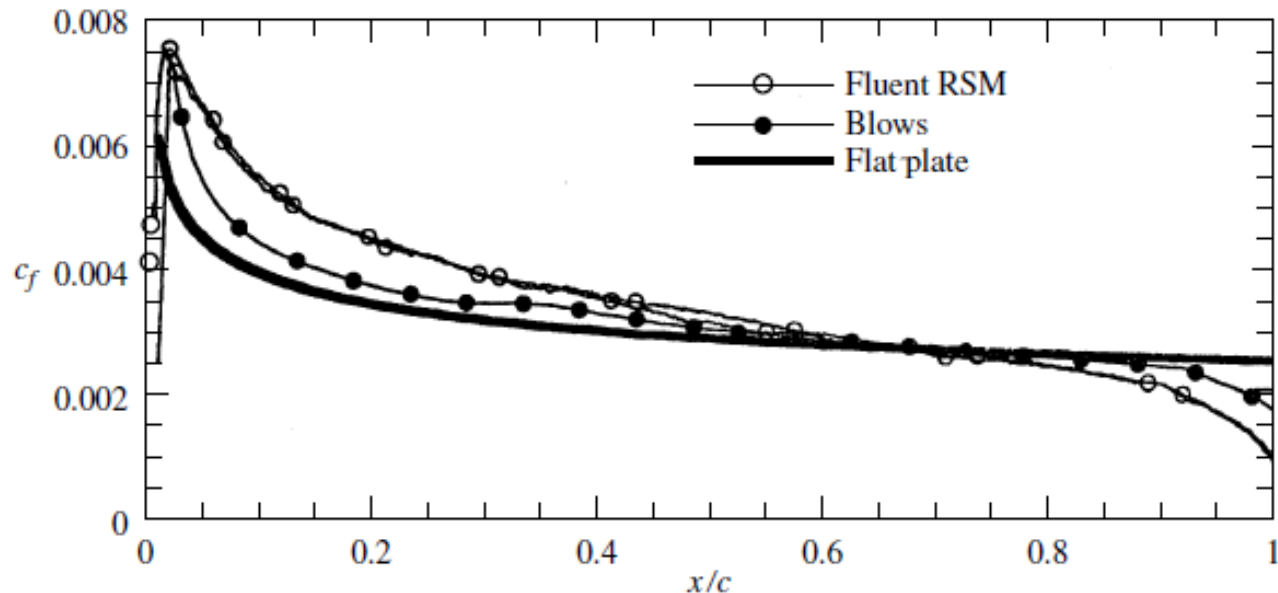


Figure 20.16 Computed skin-friction coefficient distributions over an NACA 0012 airfoil, comparing results from a Navier-Stokes solution and a boundary-layer solution. The heavy curve is for a flat plate, allowing a comparison with the skin friction distribution over a curved airfoil surface. (Data Source: Lombardi et al., Reference 92.)

第五节：小结

20.5 SUMMARY

1、粘性流动求解的一种方法：

Navier-Stokes equations 的数值计算

The solution of viscous flows

We have the following options:

1. Exact solution
2. Approximate solution
3. Direct numerical simulation

2、数值方法精度的影响因素

对于复杂流动问题（流动分离）：

- (1) 需要在近物面处布置非常密的网格
- (2) 考虑湍流模型计算精度的影响
- (3) 大多数湍流模型缺乏对转捩的预测能力